Future Journal of Pharmaceutical Sciences

RESEARCH

Open Access

Antirheumatoid arthritis and cellular uptake study of cefuroxime axetil-loaded boswellic acids nanoparticles on RAW 264.7 cells

Gitika Rani[1], Seema Rohilla[2*], Ankur Rohilla[3], Vanish Kumar[4] and Ishab Kumar[5]

Abstract

Background The present study revealed the grafting of extracted oleo gum resin of *Boswellia serrata* with polyacrylamide by conventional method with a principle of radical polymerization by using potassium per sulfate/ascorbic acid as redox initiator. A series of copolymer were synthesized using varying concentration of acrylamide at varying temperature. The optimum ratio for grafting was selected (1:2.5), on the basis of percent grafting and grafting efficiency. The grafted gum was further used as a nanocarrier to encapsulate cefuroxime axetil for their sustained release. Then, the nanoparticles were further analyzed by FT-IR, scanning electron microscopy, and DLS. The encapsulation efficiency (%), loading capacity (%) and drug content (%) was also calculated.

Result The optimized nanoparticles have shown spherical morphology with dimension of 209.4 ± 20.46 nm along with entrapment efficiency (62.47 ± 4.23%), loading capacity (33.57 ± 3.01%) and drug content (89.35 ± 6.47%). The prepared nanoparticles had found to be more stable at 4 °C. The experiential results rationalize the effectiveness of cefuroxime axetil-loaded boswellic acid nanoparticles owing to higher cellular uptake, nonstop intercellular drug withholding and improved antiproliferative effect by initiating apoptosis.

Conclusion The significant anti-arthritic effect of developed nanoparticles may be endorsed due to its dimension, encapsulation efficiency, and long-lasting drug release profile. Thus, the developed nanoparticles may assume to be a hopeful formulation for rheumatoid arthritis, which requires further investigation and may recommend a novel track to arthritis patients.

Keywords Rheumatoid arthritis, Cefuroxime axetil, Grafting, Nanoparticle, Cytotoxic

Background

Rheumatoid arthritis (RA) is systemic autoimmune disarray with symptoms of severe inflammation in joints and associated tissues [1]. Females have higher prevalence of approximately 0.24% than males [2]. Some factors like hormonal imbalance alters cortisol level, environmental factors, and lifestyle changes like androgen levels elicited by stress activated the provocative response of the body [3]. It is assumed that the incursion of provocative cells (T cells and B cells) into the synovial fluid and pannus is responsible for complete tissue devastation that leads to RA [4]. Inflammation increased the production of cytokines that damage the joints and caused synovitis, and oedema. Synovial fluid contains many immune cells

*Correspondence:
Seema Rohilla
seemarohilla4@gmail.com
[1] Department of Pharmaceutical Sciences, Geeta University, Panipat, Haryana, India
[2] Department of Pharmacy, Panipat Institute of Engineering and Technology (PIET), Smalkha, Panipat, Haryana 132102, India
[3] Department of Pharmaceutical Sciences, Universal Group of Institutions, Dera Bassi, Mohali, Punjab 140501, India
[4] National Agri-Food Biotechnology Institute, Sector-81, P.O. Manauli, S.A.S., Nagar, Mohali 140306, India
[5] Modern College of Pharmacy, Kochabhawar, Kanpur Road, Jhansi 284128, India

including monocytes, mast cells and a minute quantity of adaptive immune cells like plasma cells, Th17, Th1 (T-helper type 1), and B cells, that are implicated in the irritation. Moreover, the presence of large quantity of neutrallizers against citrullinated proteins encourages the discharge of accompaniment proteins that triggered the inception of the inflammatory effect [5, 6].

The main aim of treatment is to produce beneficial effects against joint pain, inflammation and tissue deformities to restore life's quality. The first-line drug therapies against joint soreness, inflammation and puffiness include NSAIDs, corticosteroids, and opioids. The goals of therapy include evading of further joint damage and decline in tissue deformity [7, 8]. The combination of grafted gum of *Boswellia serrata* and cefuroxime axetil is assumed to produce a synergistic effect against rheumatoid arthritis.

Cefuroxime axetil is 1-acetoxyethyl ester of a β-lactamase stable cephalosporin. Cefuroxime has pervasive activity against Gram-negative and Gram-positive microorganisms [9]. After absorption on oral use cefuroxime axetil is converted into cefuroxime on hydrolysis by estrases enzyme in intestinal mucosa and portal blood. Presence of the 1-acetoxyethylester group at position 4 of cefuroxime axetil leads to hydrophobicity and encourages the intestinal absorption of cefuroxime hence, the prodrug has shown meagre and erratic oral bioavailability (30% in fasted and 50% in fed states) [10, 11]. Out of crystalline and amorphous form of Cefuroxime axetil, amorphous form has higher bioavailability due to its better solubility [12]. Spray drying is the most successful attempt to produce amorphous cefuroxime axetil from a commercial point of view [13]. Nanoparticles are recognized to modify the dissolution rate and improved the bioaccessibility of hydrophobic drugs by augmenting the surface exposure for dissolution as described by the Noyes-Whitney equation [14]. Nanoparticles-based drug delivery is an auspicious proposal over traditional formulation and they are expected to bring a beneficial revolution in the field of medicine. Normally for the synthesis of nanoparticles synthetic material (metallic, non-metallic), semi-synthetic polymers [15] are used but due to higher immunogenicity, non-toxic nature, biodegradability and higher stability in the G.I. tract natural gums can be used as core material to encapsulate the drug [16].

Boswellia serrata, Roxburgh and other species of *Boswellia* are the natural sources of oleo gum resin. It is usually familiar as Indian frankincense or salai guggal. It contains gum (30–36%), an acid resin (boswellic acid) (56–60%), volatile oil (3–8%) and a resene (olibanoresene). The gum fraction is about one-third of Olibanum [17]. This part is soluble in water and contains polysaccharide and polymeric parts, whereas the resin part is soluble in alcohol and terpenes. Abundant studies on the natal activity of B. serrata gum-resin extract have revealed its efficacy against inflammatory diseases, such as rheumatoid arthritis, osteoarthritis [18], inflammatory bowel disease [19], cancer [20], asthma [21] and ulcerative colitis [22]. Boswellic acid has shown its activity by inhibiting enzyme 5-LOX [23] HLE [24], cathepsin G [25] and microsomal prostaglandin E2 synthase [26]. Natural gums have ability to decrease interfacial tension; this property of natural gum has shown application in stabilization/reducing nanoparticles of synthetic materials [27]. But here we consider gum as main nanocarrier for delivery of drug. Gums have property to swell its internal body act as core where the drug can be encapsulated.

Natural gums are polysaccharide in nature having different functional groups like hydroxyl, carboxyl, sulfate and amino. We can easily modify their properties and characteristics by polymerization of monomer or by combining these groups with different hydrophilic or hydrophobic molecules to make a tailor-made drug delivery system. The polymerization of monomer is called grafting [29].

The concept of grafting allows structural modification on the polysaccharides, where monomers of other polymers are covalently bonded onto the existing polysaccharide chain. It improves the structure–function relationship of natural polysaccharides by imparting a variety of functional groups onto the backbone of natural gum. A number of scientists have focused on natural gum grafting by using polymer [29, 30].

The fusion of nanotechnology and natural gum cuddles the concept of green chemistry. The green chemistry utilized the principle that decreases production of perilous substance in the proposal, manufacture and appliance of nanometric formulation. The considerable research work has seen on the resinous part of gum however, water soluble polysaccharides part of the gum getting fewer attention [31]. So in this paper we focus on aqueous soluble part. In this study, first we grafted the extracted gum with acrylomide and then encapsulated cefuroxime auxetil in their nanoparticles with aims to produce a synergistic effect against rheumatoid arthritis and to reduce joint pain, inflammation and tissue deformities.

Methods

Cefuroxime axetil was gifted by rachil pharma, talwar, Punjab, India. Acrylamide, Methanol, DMF (CDH), and Potassium per sulfate were purchased from Central Drug House (P) Ltd, New Delhi, India. Ascorbic acid and PBS were procured from Sigma-Aldrich, MO, USA. *Boswellia serrata* gum purchased from local markets of Rohtak, India. The murine macrophage cell line RAW 264.7 was received from the National Cell Repository of National Center for Cell Science, Pune, India. All ingredients used in study were of analytic quality.

Preparation of acrylamide grafted extracted B. serrata gum

Boswellia serrata (oleo gum resin-raw sample) powder (25gm) was added in 200 ml deionised water and stirred at 800 rpm overnight at room temperature. Then, this combination was centrifuged for 10 min at 1500 rpm and the supernate was collected. Thereafter, the supernate was again centrifuged (Sigma ultracentrifuge 3-30KS; SciQuip Ltd., Germany) at 2500 rpm for 10 min and successively at 10,000 rpm for 20 min, and then filtered. Then, the filtrate was freeze-dried to − 80 °C and 0.25 torr for 24 h. Then, the freeze-dried sample was deliquesced in 100 ml methanol and stirred at 500 rpm for 12 h at room temperature and placed for 1 h separately without disturbing. Then, the observed precipitate was collected and dried in oven at 50°C. This extracted gum was used further for grafting [32].

Grafting of acrylamide on extracted *Boswellia serrata* gum was done by conventional heat assisted method. Known amount of powdered gum and acrylamide were dissolved in 25 ml at temperature between 50 to 70 °C. 5 mg of ascorbic acid was added in the above solution. After 10 min, 10 mg potassium per sulfate (KPS) was added and retained the sample at same temperature for 1 h. KPS promoted the main chain degradation and lowered grafting percentage and acrylamide conversion on further increase in concentration due to O_2 formation. To complete grafting reaction, the sample was kept undisturbed for 24 h. The observed gel like mass was poured into 50 ml of acetone. The precipitate formed were collected and dried at 50 °C in hot air oven and used for further experiment [16, 33].

Different batches of formulation were designed to evaluate their percent grafting and grafting efficiency. The batches were prepared on the basis of increasing value of the variables (i.e. increasing ratio and amount of acrylamide from G1 to G5 and batch G6 and G7 were prepared with same ratio (1:1) and with different temperatures than other batches to evaluate the effect of temperature on percent grafting and grafting efficiency. The batch of grafted gum having maximum percent grafting and grafting efficiency was used to prepare nanoparticles.

Evaluation of grafting efficiency

Percent grafting and grafting efficiency of different batches were calculated by using following equations [34]:

$$\text{Percent grafting} = \frac{(W_1 - W_0)}{W_0} \times 100$$

$$\text{Grafting Efficiency (\%)} = \frac{(W_1 - W_0)}{W_2} \times 100$$

where W_0 is weight of gum, W_1 is weight of grafted copolymer and W_2 is weight of acrylamide.

Preparation of cefuroxime axetil encapsulated grafted *Boswellia serrata* nanoparticles

The nanoparticles of grafted oleo gum resin of B. serrata containing cefuroxime axetil were formulated by the solvent displacement technique. The batch of grafted gum having maximum percent grafting and grafting efficiency was used to prepare nanoparticles. It was stirred in 45 ml of deionized water for 3 h. Cefuroxime axetil (80 mg) was stirred in 5 ml of DMF for 3 h. The solution was mixed with copolymer solution at 37°C. The mixture was stocked in dark at 40°C for 24 h. The mixture was lyophilized (Spscienmac) and centrifuge (Sigma ultracentrifuge 3-30KS; SciQuip Ltd., Germany) with water at 10,000 rpm. The pellet was again freeze dried and dried material was collected and analyzed by high-performance liquid chromatography (HPLC) (Agilent technologies 1200 series, Germany) [35].

Characterization of nanoparticles

Entrapment efficiency, drug content and loading capacity

Entrapment efficiency and drug content in formulation were quantitatively determined after breaking of the prepared nanoparticles with alcohol followed by sonication for 10 min. The supernatant was properly mixed by using magnetic stirrer and then 5 ml of supernatant was taken and filtered. The content of the drug was analyzed using HPLC (1200 series, Agilent Technologies, Germany). The analysis of sample was performed in triplicate. The sample was introduced by a microsyringe and examined at 281 nm [36]. The drug loading, drug content and encapsulation efficiency were calculated with following formulas:

$$\text{Entrapment efficiency (\%)} = \frac{\text{Total amount of drug} - \text{concentration of supernatant drug}}{\text{Total amount of drug added}} \times 100$$

$$\text{Drug content (\%)} = \frac{\text{Amount of drug entrapped}}{\text{Amount of nanoformulation taken}} \times 100$$

$$\text{Loading Capacity (\%)} = \frac{\text{Total drug} - \text{Free drug}}{\text{Lipid Content } \left(\text{Grafted gum}\right)} \times 100$$

FT-IR spectral analysis

The FT-IR spectra of aqueous extracted gum and acrylamide grafted gum of *Boswellia serrata*, cefuroxime axetil encapsulated in nanoparticles composed of grafted gum of *Boswellia serrata* were recorded on FT-IR spectrophotometer (FT-IR-Alpha Bruker 1206 0280, Germany) by KBr disc method [36]. The samples were mulled with dried KBr powder and compressed into a compact disc. The sample scanned at a resolution of 4 cm^{-1} from 400 to 4000 cm^{-1} after positioned the sample in sample holder.

Scanning electron microscope (SEM)

Sample of extracted gum, grafted gum and nanoparticles was prepared on double sided carbon tape and mounted on to the stub and then fine coat ion sputter is used to make a fine coating of gold palladium alloy (150-200Å). The sample was analyzed under the scanning electron microscope (Jeol 6000) to study external morphology of particles [37].

Dynamic light scattering

The zetasizer nano series Nano-ZS90 (Malvern Instruments, Malvern, UK) equipped with the hydro dispersing unit was used to determine the dimension and the size distribution of extracted gum, grafted gum, cefuroxime axetil encapsulated nanoparticles. All samples were prepared in water in concentration 0.3 mg/ml. The sample was poured in a polystyrene cuvette of hydro dispensing unit and observed at 25 °C with 10 runs in 50 s. After scanning, the mean diameter was reported [38].

In-vitro drug release

In-vitro release of cefuroxime axetil loaded nanoparticles composed of acrylomide grafted gum of *Boswellia serrata* (CA-NGG) were estimated via the dialysis bag diffusion technique at gastric pH 1.2 and phosphate buffer pH 6.8. A preset quantity of CA-NGG (100 mg) was relocated to dialysis membrane (Himedia, Mumbai, India) (specification: average flat width = 32.34 mm, average diameter = 21.5 mm, capacity = 3.63 ml/cm^2, molecular weight cut-off = 12,000 Da) bag and sealed both ends of bag. The United State Pharmacopoeia (USP) dissolution apparatus II (Lab India DS 8000, Mumbai, India) was used to conduct *in-vitro* release studies. The dialysis bag containing CA-NGG was positioned in the dissolution medium sustained at 37 °C ± 0.5 °C. Then, the sample was withdrawn at preset intervals (0.5, 1, 2, 4, 6, 8, 12, 18, 24 h), and replaced with fresh media. The samples were analyzed by HPLC at 281 nm in triplicate [39].

In-vitro cell line study

Cellular intake assay To evaluate the cellular intake efficiency of GG and CA-NGG, the non-polar infrared fluorescent dye DiD was entrapped in GG and CA-NGG. RAW 264.7 cells were sowed in 12-well plates (1×10^5 cells per well) for a day and divided in two groups i.e. pre-treated or not pre-treated. They were treated with lipopolysaccharide (2 µg/ml) for 4 h and washed with phosphate buffer saline thrice. Then, the cells were gestated with GG/DiD and CA-NGG/DiD (an equivalent dose of 0.5 µg/ml of DiD) for an additional 0.5 h and 2 h. Then, the cells were washed thrice with fresh phosphate buffer saline after removing the medium and then again harvested. The extent of fluorescence due to DiD in the cells was analyzed by flow cytometry (BD FACSCelesta, San Jose, CA). To determine the uptake of lipopolysaccharide-activated RAW 264.7 cells qualitatively, the cells were sowed in glass bottom dishes (2×10^4 cells per dish) and activated with lipopolysaccharide as explained previously. The cells were kept in 4% paraformaldehyde for 20 min, after being incubated with GG/DiD and CA-NGG/DiD for 0.5 and 2 h. Then, the cells were stained with DAPI for 5 min. The samples were then studied by laser scanning confocal microscopy (LSCM, LSM 800, Zeiss, Oberkochen, Germany) [40, 41]. The cellular intake was expressed as the amount (ng) of the CA-NGG and GG allied with a unit weight (mg) of cellular protein.

Cytotoxicity studies The cytotoxicity of GG and CA-NGG was examined using RAW 264.7 cells. The medium to harvest cell was consisted of 10% fetal bovine serum (FBS) and 90% Dulbecco's modified eagle's medium (DMEM). The MTT test was selected to study cell cytotoxicity. The hemocytometer and the trypan blue exclusion method were used to find out the number of viable cells in the cell suspension. For test, the cells (5×10^3 cells/well) were seeded in each well of a 96-well culture plate for 1 day in an incubator at 37 °C with 5% CO_2 saturated humidity. On the subsequent day, the medium was substituted with suspension of GG and CA-NGG prepared in 10 ml of DMEM medium in different concentrations like 50, 100, 150, 250, 500, and 750 nM. After 2 days, the medium containing suspensions was removed and then the MTT test was performed after washing with phosphate buffer saline. The cell viability was assessed at 570 nm with a reference wavelength of 630 nm using an ELISA microplate reader (Biotek, Winooski, VT) in triplicate, and the results were reported as the means ± SDs [42].

Influence on generation of TNF-α This study helped to determine how GG and CA-NGG influenced RAW 264.7 cells capability to produce TNF-α (obtained from the blood of mouse). Complement media for cells contained DMEM + 2 mM glutamine + 10% phosphate buffer saline. A sandwich ELISA kit was utilized to estimate the

quantity of TNF-α produced in cell lysates. The cells were sowed in 24 well plates at a density of 2×10^5 cells per well, then nurtured with GG and CA-NGG for 2 h. Lipopolysaccharide (1 µg/ml) was used to activate the cells for 24 h and then the absorbance was recorded at 450 nm on an ELISA microplate reader (Biotek, Winooski, VT, USA) in thrice, and the data were reported as a mean ± SD [43].

Stability studies

For 3 months, CA-NGG formulations were stocked under different conditions like at cool temperature (4 ± 2 °C), room temperature (25 ± 2 °C), and accelerated temperature (45 ± 2 °C) to evaluate their stability. Entrapment efficiency (EE), particle size (PS), and physical appearance were estimated at interval of 1 month for 3 months to confirm the alterations in physical and chemical properties of formulation [44].

Results

Preparation and characterization of Acrylamide grafted *Boswellia serrata* gum

Grafting efficiency

Boswellia serrata gum (Olibanum gum) extracted from *Boswellia serrata*. The grafting gum was synthesized using a different acrylamide concentration (Table 1). The results evidenced that the percent grafting increased with increase in acrylamide concentration and the percent grafting efficiency was also enhanced with rise in temperature. Batch G5 was selected as optimum to prepare nanoparticles on the basis of maximum percent grafting and grafting efficiency.

Entrapment efficiency, drug content and loading capacity

Entrapment efficiency, drug content and loading capacity of nanoparticles prepared by using composition of batch G5 are shown in Table 2.

FT-IR spectral analysis

The FT-IR spectra of extracted gum, acrylamide grafted gum and optimized formulation were shown in Fig. 1. In

Table 2 Entrapment efficiency, drug content and loading capacity of cefuroxime axetil encapsulated nanoparticles composed of acrylomide grafted gum of *Boswellia serrata* (Batch G5)

S. no.	Parameters	Values
1	Entrapment efficiency (%)	62.47 ± 4.23
2	Loading capacity (%)	33.57 ± 3.01
3	Drug content (%)	89.35 ± 6.47
4	Particle size (nm)	209.4 ± 20.46

FT-IR spectrum of acrylamide grafted gum of *Boswellia serrata*, a pointed intense peak at 1646 cm^{-1} with a miniature band and a peak at 1601 cm^{-1} depicted the N–H in-plane bending of $–CONH_2$ group and C=O stretching of amide I band, respectively, that confirm the copolymerization of extracted gum with acrylamide. The small peaks at 1418 cm^{-1} and 1391.2 cm^{-1} demonstrated N–H bending and C–N stretching indicated the grafting of copolymerization of acrylamide on gum of *Boswellia serrata*. The peak at 3338 cm^{-1} and 3186.3 cm^{-1} showed shifting of peaks of gum evidenced some bond formation on gum structure.

Morphological characterization

The images depicted the spherical shape and smooth morphology of nanoparticles having dimension in nanorange (Fig. 2). SEM image of aqueous extracted gum has shown the rough morphology of gum that indicated its porous structure.

Dynamic light scattering

Dynamic light scattering analyses have shown the diameter of about 327 nm in aqueous extracted *Boswellia* gum. The intensity of the peak was 83.5%. The DLS analysis of copolymer found approx. 259.3 nm and intensity was 91.9%. DLS of the nanoparticles was found near 209 nm and intensity of peak 92%. PDI 0.641 revealed the monodispersive nature of particles.

Table 1 Percent grafting and grafting efficiency of different batches

Batch	Ratio (G:A)	Temperature (C)	Gum (mg)	Acrylamide (mg)	Ascorbic acid (mg)	KPS (mg)	% Grafting	Grafting efficiency (%)
G1	1:05	70	400	200	5	20	16	32 ± 0.85
G2	1:1	70	400	400	5	20	63.7	63.7 ± 1.43
G3	1:1.5	70	400	600	5	20	102.9	68.6 ± 0.98
G4	1:2	70	400	800	5	20	142.8	71.4 ± 1.23
G5	**1:2.5**	**70**	**400**	**1000**	**5**	**20**	**183.7**	**73.5 ± 1.18**
G6	1:1	50	400	400	5	20	30	30.2 ± 0.7
G7	1:1	60	400	400	5	20	56.05	56 ± 0.4

Boldface depicted the optimum batch, that we selected for for further experiment

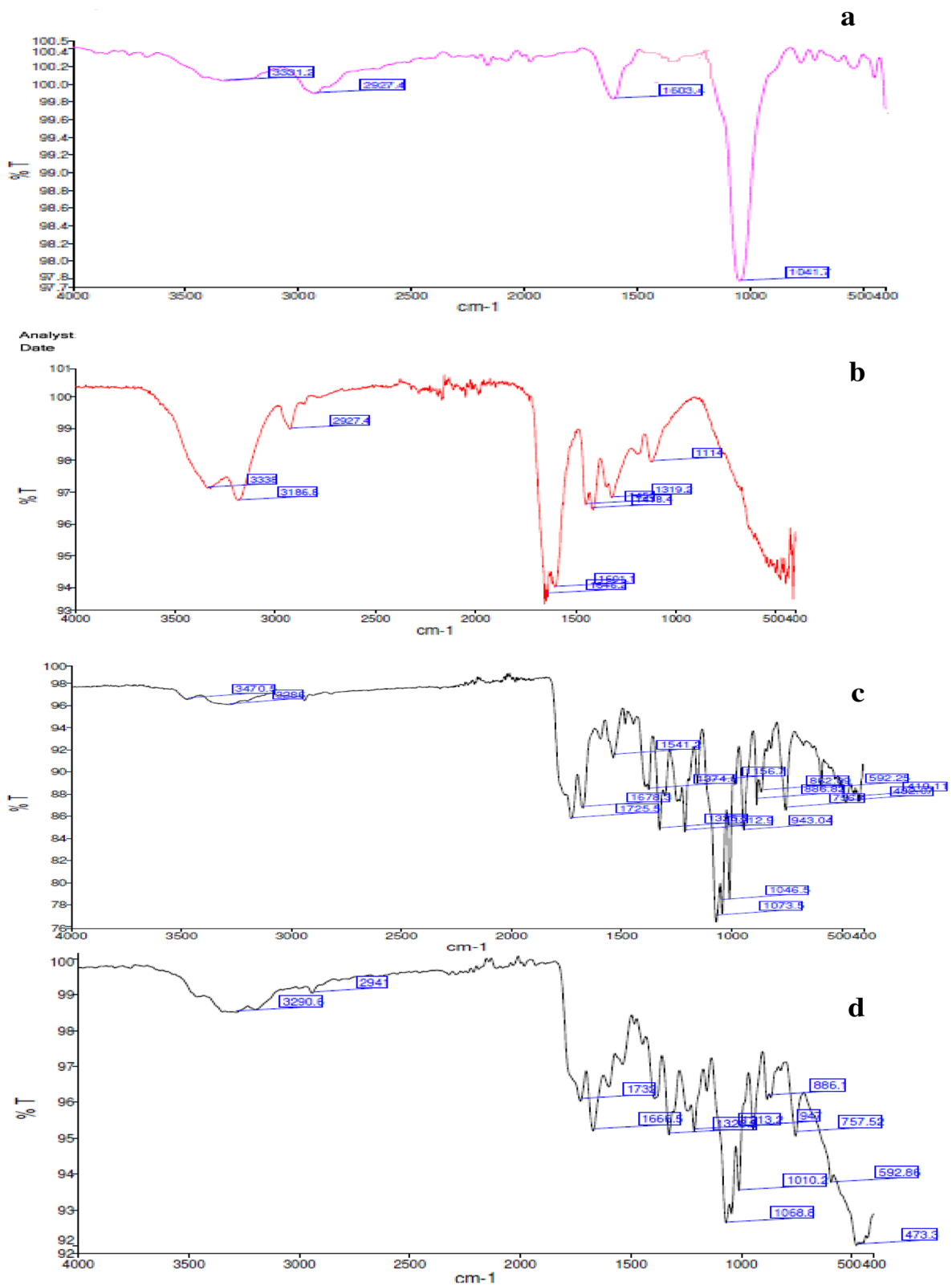

Fig. 1 FT-IR Spectra of **a** extracted gum, **b** acrylamide grafted gum, **c** cefuroxime axetil, **d** cefuroxime axetil encapsulated grafted *Boswellia serrata* nanoparticles

In-vitro drug release

In-vitro drug release of CA-NGG was estimated by the dialysis bag diffusion technique. Optimum batch of CA-NGG contain gum and acrylomide in ratio 1:2.5. The average of % cumulative drug discharge of optimum batches was found to be 88.77 ± 3.024% and 59.47 ± 3.17% in phosphate buffer pH 6.8 and in gastric pH 1.2 respectively after 24 h (Fig. 3).

The results from release kinetics demonstrated that the drug followed Higuchi dispersion model to discharge from the nanoparticles having value of relapse coefficient (0.994). The values of correlation coefficient for zero order, first order, Higuchi's release model, and Korsemeyer-Peppas's model were found as 0.982, 0.984, 0.994, and 0.969, respectively. The value of diffusion exponent 'n' of the Korsmeyer-Peppas equation was 0.85 ($0.5 \leq n \leq 0.8$) which demonstrated incoherent diffusion or Non-Fickian diffusion mechanism for drug liberation [36, 39].

Cellular uptake and anti-inflammatory competence of nanoformulations of acrylamide grafted gum of *Boswellia serrata*

The level of grafted gum (GG) and CA-NGG on LPS-activated cells was investigated by using an immunofluorescent stain. The outcomes of flow cytometry and LSCM depicted that the uptake of both GG/DiD and CA-NGG/DiD is augmented in a time-dependent manner both by normal RAW 264.7 cells (LPS-) and LPS-activated RAW 264.7 cells (LPS+) (Fig. 4). Distinctively, the fluorescence intensity of CA-NGG/DiD 2.9 times higher after 120 min than that of GG/DiD and was 2.1 times higher at 30 min when RAW 264.7 cells were activated with LPS. The results depicted that in macrophages activated cells, the cellular uptake efficiency of CA-NGG/DiD was better than that of GG/DiD at the selected time intervals due to the specific interaction between acrylomide and extracted gum [45].

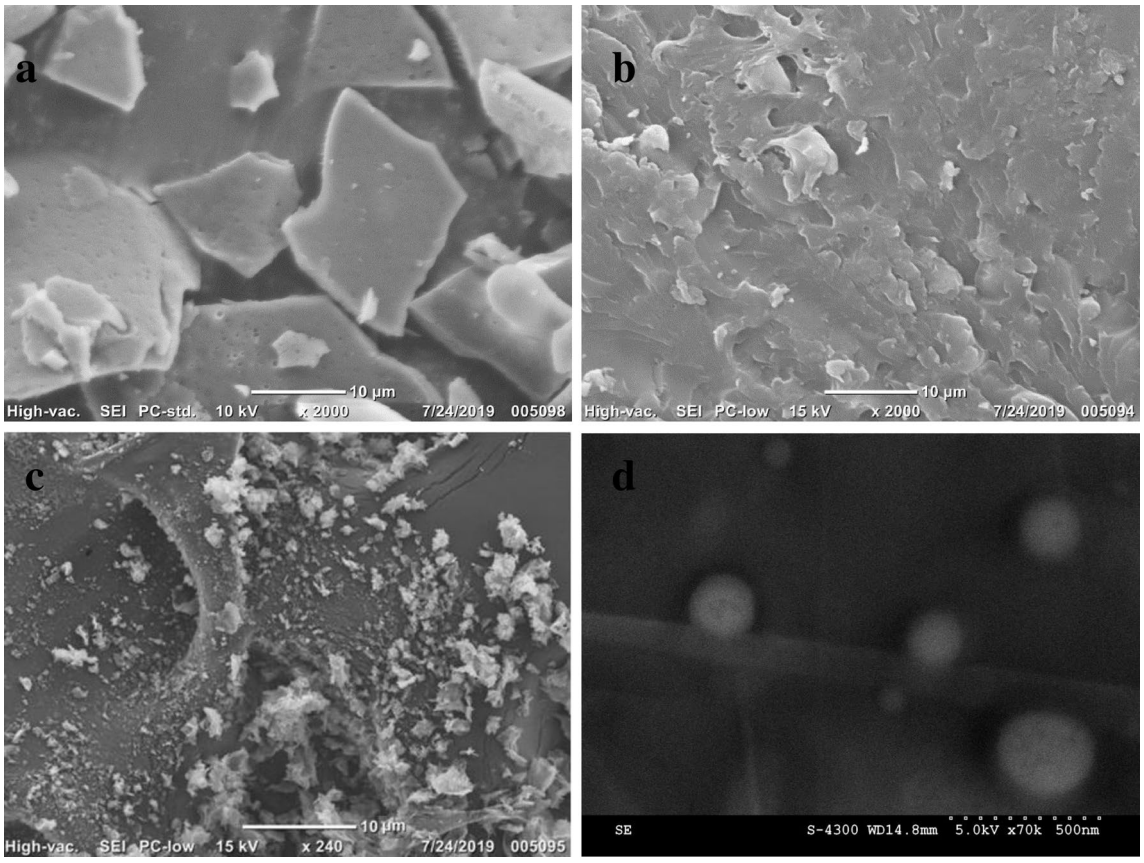

Fig. 2 SEM images of **a** extracted gum, **b** acrylamide grafted gum, **c, d** cefuroxime axetil encapsulated grafted *Boswellia serrata* nanoparticles

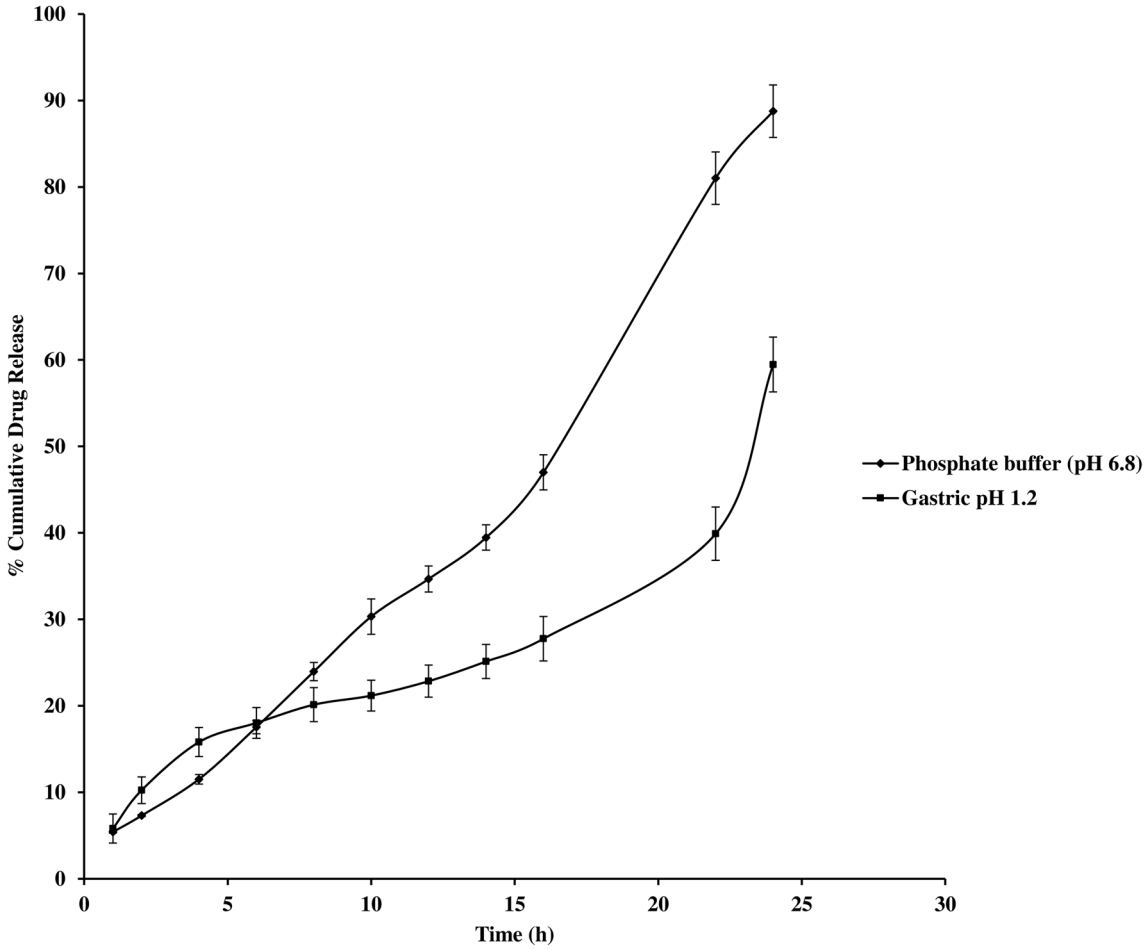

Fig. 3 Cumulative drug release of cefuroxime axetil from nanoformulations of acrylamide grafted gum of *Boswellia serrata*

Influence on TNF-α generation

TNF-α is vital for the development and intensification of fibroblasts and for the initiation of pro-inflammatory intermediates in pathogenesis of rheumatoid arthritis. As a consequence, it persuades synovitis and initiates the damage of cartilage and bone. CA-NGG treatment declined the TNF-α production of RAW 264.7 cells significantly than free GG. The outcome recommended that the anti-arthritic characteristics of the CA-NGG restrained the generation of inflammatory cytokines like TNF-α. Decreased production of TNF-α is allied with less cartilage damage and inflammation, which can arrest the progress of arthritis.

Cytotoxicity study

The MTT (3-(4,5-dimethylthiazol-2-yl)-2,5-diphenyl tetrazolium bromide) assay was used to assess the cell viability of the macrophage cell line RAW 264.7 against GG and CA-NGG. The cell viability of RAW 264.7 cells in variable amounts of GG and CA-NGG was found to be 95.79% to 34.21% (Fig. 5). The outcomes depicted that the possibility of RAW 264.7 cells declined in direct proportion to the quantity of GG and CA-NGG.

Stability studies

To confirm the stability of CA-NGG, the stability studies of the nanoformulation were performed at 4 °C, 25 °C and 45 °C for 3 months (Table 3). The entrapment efficiency and particle size altered drastically during storage at 25 °C and 45 °C. The probable mechanism for this alteration will be the polymorphic conversion of cefuroxime axetil. No major change in dimension and entrapment efficiency was noticed at 4 °C. This indicates that CA-NGG nanoformulation was found to be more stable at 4 °C.

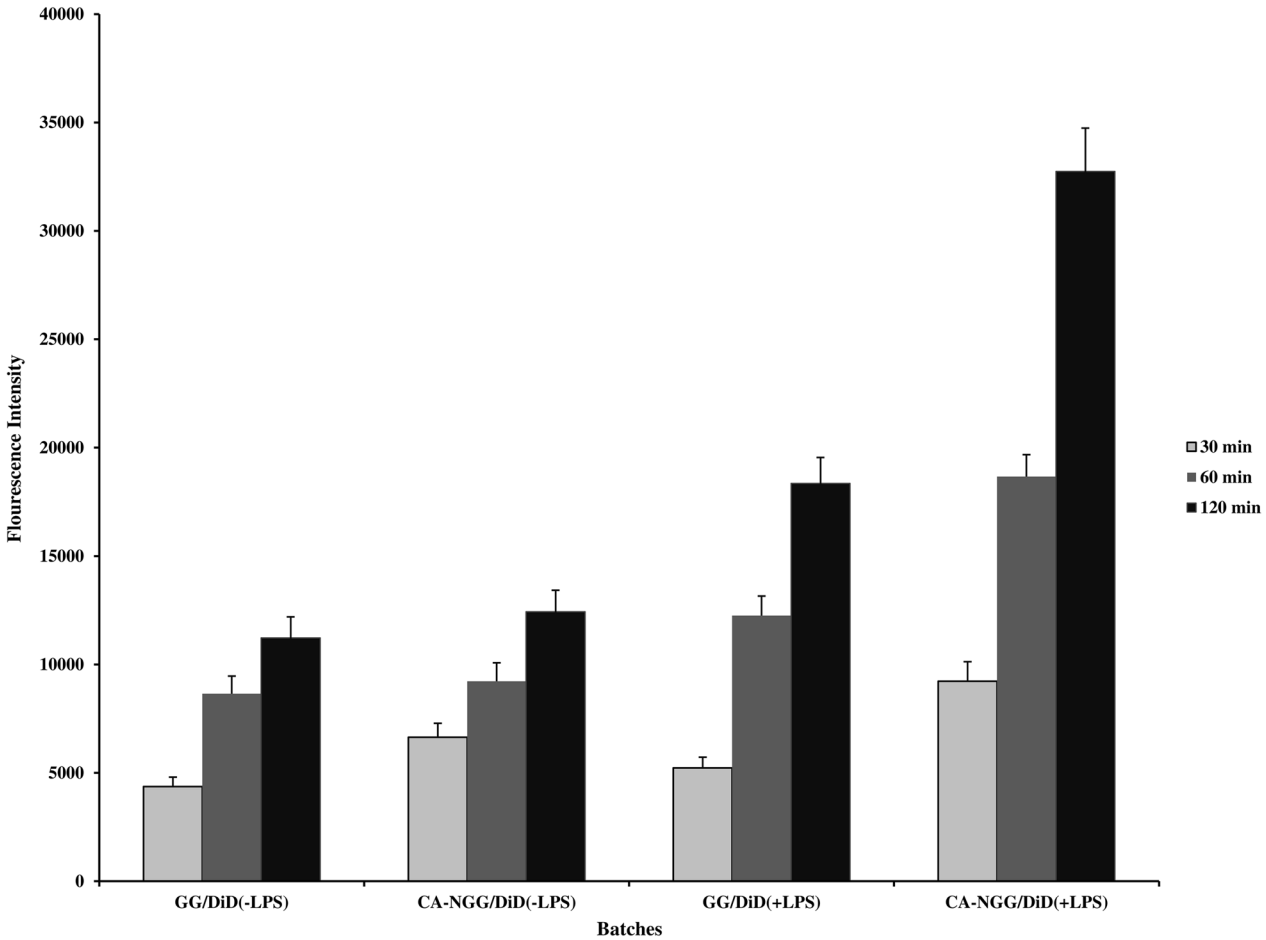

Fig. 4 Cellular uptake of nanoformulations of acrylamide grafted gum of *Boswellia serrata* on LPS-stimulated cells by immunofluorescence staining

Discussions

The grafting gum was synthesized using a different acrylamide concentration and on the basis of maximum percent grafting and grafting efficiency batch G5 was selected for further studies. Compatibility between drug and acrylamide grafted gum was estimated using FT-IR spectroscopy. The occurrence of diverse functional groups and bandwidth were analyzed to examine even minor amendments in the arrangement. The peaks in FT-IR spectra were revealed that the aqueous extracted gum from *Boswellia serrata* oleo gum resin did not have any peak of methoxy group. FT-IR of nanoparticles showed that the drug was encapsulated in copolymer. Neither shifting/overlapping of functional peaks nor significant new peaks were noticed in case of optimized nanoformulation in contrast to the spectrum of the pure drug and acrylamide grafted gum of *Boswellia serrata*. The outcomes evidenced the stability of drug during encapsulation and did not designate any interaction between drug and acrylamide grafted gum of *Boswellia serrata*. Bairwa and Jachak, developed a poly-DL-lactide-co-glycolide-based nanoparticle formulation of KBA (11-keto-b-boswellic acid) to improve its oral bioavailability and *in-vivo* anti-inflammatory activity and confirmed their results [46]. Soumya et al. prepared guar gum nanoparticles by cross-linking and nanoprecipitation method to be used as carriers for different formulations [47].The SEM images of grafted gum and copolymer were depicted their smoother, less porous and uniform surface than extracted gum. The results from DLS demonstrated that the size of the copolymer was decreased as compared to aqueous extracted gum. The nanoparticles have shown higher cumulative release of cefuroxime axetil in phosphate buffer pH 6.8 than acidic pH after 1 day and follow a persistent discharge prototype. The release kinetics

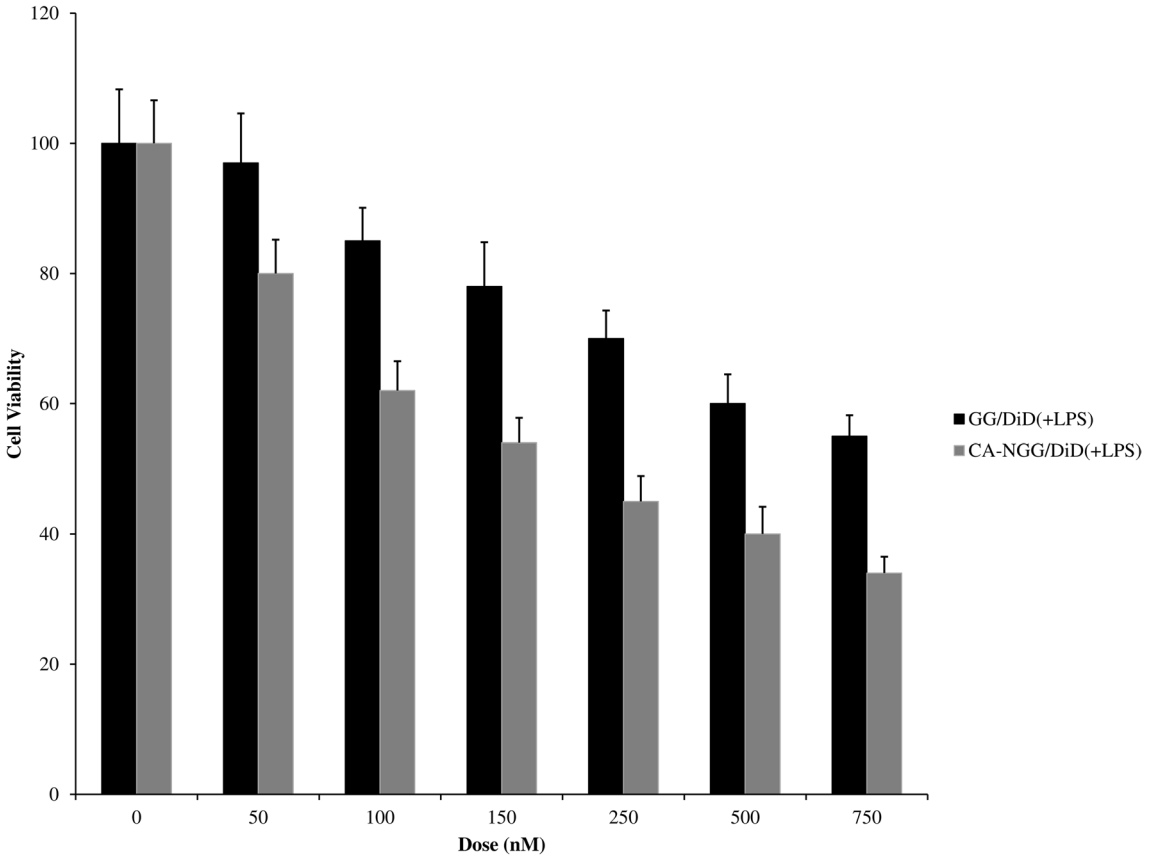

Fig. 5 Cytotoxicity study of GG and CA-NGG in LPS-stimulated RAW 264.7 cells

studies demonstrated that the drug follow Non-Fickian diffusion mechanism to liberate from the nanoparticles. The nanoformulations were found to be more stable at 4 °C. Farooq et al. prepared microgels using gum Arabic by reverse micellization method and evaluated their efficacy and compatibility with blood [48]. Aamir et al. prepared gum arabic-based spherical microgels by reverse micellization method and observed the yield of about 79% in 5–50 µm size range [49]. LSCM and flow cytometry were used to evaluate the cellular uptake efficiency of the grafted gum (GG) and nanoparticles (CA-NGG) by RAW 264.7 cells. DiD was used as a luminescent probe. The results depicted that in macrophages activated cells, the cellular uptake efficiency of CA-NGG/DiD was better than that of GG/DiD due to the specific interaction between acrylomide and extracted gum. CA-NGG restrained the generation of TNF-α. Decreased production of TNF-α is allied with less cartilage damage and inflammation, which can arrest the progress of arthritis. The viability of RAW 264.7 cells were declined in direct proportion to the quantity of GG and CA-NGG. Thus, the higher dose of nanoformulations induced much cell cytotoxicity than free GG.

Conclusions

In the present study, we grafted acrylamide on extracted gum of *Boswellia serrata* and encapsulated cefuroxime auxetil drug in acrylamide grafted *Boswellia serrata* gum nanoparticles by the solvent displacement technique. The optimized nanoparticles formulations were found to have synergistic effects in the treatment of asthma, sinusitis and bronchitis, as well as lung-throat issues with coughing and wheezing. The grafting efficiency was increased with the elevation in acrylamide amount as well as temperature. The nanoparticles have shown good entrapment efficiency, drug content and loading capacity. The acrylamide grafted nanoparticles give a good prospective for sustained drug delivery preparation as it offered protective covering to the entrapped materials against the chemical alterations.

Table 3 Outcomes of stability studies of optimized CA-NGG nanoformulation

Time	0 Month			1 Month			2 Month			3 Month		
Parameter	**4 °C**	**25 °C**	**45 °C**	**4 °C**	**25 °C**	**45 °C**	**4 °C**	**25 °C**	**45 °C**	**4 °C**	**25 °C**	**45 °C**
EE (%)	62.47 ± 4.23	62.47 ± 4.23	62.47 ± 4.23	61.87 ± 5.45	52 ± 4.68	49 ± 3.98	60.43 ± 6.09	48 ± 4.51	30 ± 2.56	59.45 ± 5.34	30 ± 2.16	15 ± 1.03
Particle size (nm)	209.4 ± 20.46	209.4 ± 20.46	209.4 ± 20.46	215.6 ± 20.98	240.67 ± 21.45	320.98 ± 5.43	221.9 ± 20.24	310.67 ± 29.68	874.09 ± 70.98	235.79 ± 20.89	490.9 ± 30.98	3065.57 ± 210.98
Physical appearance	Clear	Clear	Clear	Clear	Cloudy to slightly light yellow	Pastel yellow with small bunches of particles discrete on shaking	Clear	Pastel yellow with small bunches of particles discrete on shaking	Brownish color formulation with bunches do not discrete on shaking	Cloudy to slightly light yellow	Brownish color suspension with bunches of particles discrete on shaking	Brownish color formulation with bunches do not discrete on shaking

Nanoparticles were found to be stable at 4 °C. The formulations have modified pharmacokinetics profile as it alleviated systemic side effects and improves the therapeutic efficacy. Thus, the formulated cefuroxime auxetil loaded *Boswellia serrata* gum nanoparticles can be suggested as an appropriate drug carrier for efficient drug targeting.

Abbreviations

RA	Rheumatoid arthritis
Th1	T-helper type 1
NSAIDs	Non-steroidal anti-inflammatory drugs
G.I. tract	Gastrointestinal Tract
5-LOX	5-Lipoxygenase
HLE	Human leukocyte elastase
CDH	Central Drug House
DMF	Dimethylformamide
HPLC	High-performance liquid chromatography
CA-NGG	Cefuroxime axetil loaded nanoparticles composed of acrylomide grafted gum of *Boswellia serrata*
GG	Grafted gum
DiD	1,1-Dioctadecyl-3,3,30,30-tetramethyl indodicarbocyanine
DAPI	4′,6-Diamidino-2-phenylindole
MTT	3-(4,5-Dimethyl thiazolyl-2)-2, 5-diphenyltetrazolium bromide)
DMEM	Dulbecco's modified eagle's medium with high glucose
KPS	Potassium per sulphate

Acknowledgements
Not applicable.

Author contributions
VK, IK contributed to the design of the study; GR performed the experiments and analysis the data; SR and AR drafted the paper; all authors have read and approved the final manuscript.

Funding
No funding was obtained for this study.

Availability of data and materials
The data supporting the findings of this research article is available with corresponding author, upon reasonable request.

Declarations

Ethics approval and consent to participate
Not applicable.

Consent for publication
Not applicable.

Competing interests
The authors declare that they have no competing interests.

Received: 18 April 2023 Accepted: 10 October 2023
Published online: 27 October 2023

References

1. Guo Q, Wang Y, Xu D, Nossent J, Pavlos NJ, Xu J (2018) Rheumatoid arthritis: pathological mechanisms and modern pharmacologic therapies. Bone Res 6:15. https://doi.org/10.1038/s41413-018-0016-9
2. Cross M, Smith E, Hoy D, Carmona L, Wolfe F, Vos T, Williams B, Gabriel S, Lassere M, Johns N, Buchbinder R, Woolf A, March L (2014) The global burden of rheumatoid arthritis: estimates from the global burden of disease 2010 study. Ann Rheum Dis 73(7):1316–1322. https://doi.org/10.1136/annrheumdis-2013-204627
3. Gibofsky A (2014) Epidemiology, pathophysiology, and diagnosis of rheumatoid arthritis: a synopsis. Am J Manag Care 20(7 Suppl):S128–S135
4. Kahlenberg JM, Fox DA (2011) Advances in the medical treatment of rheumatoid arthritis. Hand Clin 27(1):11–20. https://doi.org/10.1016/j.hcl.2010.09.002
5. Chauhan K, Jagmohan SJ, Mohammed AA (2019) Rheumatoid arthritis, StatPearls [Internet]; StatPearls Publishing: Treasure Island, FL, USA. https://www.ncbi.nlm.nih.gov/books/NBK441999/. Accessed 10 April 2023
6. Suresh P, Salem-Bekhit MM, Veedu HP, Alshehri S, Nair SC, Bukhari SI, Viswanad V, Taha EI, Sahu RK, Ghoneim MM, Elbagory I (2022) Development of a novel methotrexate-loaded nanoemulsion for rheumatoid arthritis treatment with site-specific targeting subcutaneous delivery. Nanomaterials (Basel) 12(8):1299. https://doi.org/10.3390/nano12081299
7. Bullock J, Rizvi SAA, Saleh AM, Ahmed SS, Do DP, Ansari RA, Ahmed J (2018) Rheumatoid arthritis: a brief overview of the treatment. Med Princ Pract 27(6):501–507. https://doi.org/10.1159/000493390
8. Rajitha P, Biswas R, Sabitha M, Jayakumar R (2017) Methotrexate in the treatment of psoriasis and rheumatoid arthritis: mechanistic insights, current issues and novel delivery approaches. Curr Pharm Des 23(24):3550–3566. https://doi.org/10.2174/1381612823666170601105439
9. Jelinska A, Dudzińska I, Zajac M, Oszczpowicz I (2006) The stability of the amorphous form of cefuroxime axetil in solid state. J Pharm Biomed Anal 41(3):1075–1081. https://doi.org/10.1016/j.jpba.2006.02.008
10. Harding SM, Williams PE, Ayrton J (1984) Pharmacology of cefuroxime as the 1-acetoxyethyl ester in volunteers. Antimicrob Agents Chemother 25(1):78–82. https://doi.org/10.1128/AAC.25.1.78
11. Jewesson PJ (1995) Pharmaceutical, pharmacokinetic and other considerations for intravenous to oral stepdown therapy. Can J Infect Dis 6:11A-16A. https://doi.org/10.1155/1995/975209
12. Garbacki P, Tezyk A, Zalewski P, Jelinska A, Paczkowska M, Talczyńska A, Oszczapowicz I, Cielecka-Piontek J (2014) Assay of diastereoisomers of cefuroxime axetil in amorphous and crystalline forms using UHPLC-DAD. Chromatographia 77(21–22):1489–1495. https://doi.org/10.1007/s10337-014-2773-y
13. Dhumal RS, Biradar SV, Yamamura S, Paradkar AR, York P (2008) Preparation of amorphous cefuroxime axetil nanoparticles by sonoprecipitation for enhancement of bioavailability. Eur J Pharm Biopharm 70(1):109–115. https://doi.org/10.1016/j.ejpb.2008.04.001
14. Dizaj SM, Vazifehasl Zh, Salatin S, Adibkia Kh, Javadzadeh Y (2015) Nanosizing of drugs: effect on dissolution rate. Res Pharm Sci 10(2):95–108
15. Dalmoro A, Bochicchio S, Nasibullin SF, Bertoncin P, Lamberti G, Barba AA, Moustafine RI (2018) Polymer-lipid hybrid nanoparticles as enhanced indomethacin delivery systems. Eur J Pharm Sci 121:16–28
16. Kathe N, Henriksen B, Chauhan H (2014) Physicochemical characterization techniques for solid lipid nanoparticles: principles and limitations. Drug Dev Ind Pharm 40(12):1565–1575
17. Greve HL, Kaiser M, Brun R, Schmidt TJ (2017) Terpenoids from the oleo-gum-resin of *Boswellia serrata* and their antiplasmodial effects *in-vitro*. Planta Med 83(14–15):1214–1226. https://doi.org/10.1055/s-0043-116943
18. Wang Q, Pan X, Wong HH, Wagner CA, Lahey LJ, Robinson WH, Sokolove J (2014) Oral and topical boswellic acid attenuates mouse osteoarthritis. Osteoarthr Cartil 22(1):128–132. https://doi.org/10.1016/j.joca.2013.10.012
19. Siddiqui MZ (2011) *Boswellia serrata*, a potential antiinflammatory agent: an overview. Indian J Pharm Sci 73(3):255–261. https://doi.org/10.4103/0250-474X.93507
20. Agrawal SS, Saraswati S, Mathur R, Pandey M (2011) Antitumor properties of Boswellic acid against Ehrlich ascites cells bearing mouse. Food Chem Toxicol 49(9):1924–1934. https://doi.org/10.1016/j.fct.2011.04.007
21. Gupta I, Gupta V, Parihar A, Gupta S, Ludtke R, Safayhi H, Ammon HP (1998) Effects of *Boswellia serrata* gum resin in patients with bronchial asthma: results of a double-blind, placebo-controlled, 6-week clinical study. Eur J Med Res 3(11):511–514
22. Gupta I, Parihar A, Malhotra P, Gupta S, Ludtke R, Safayhi H, Ammon HP (2001) Effects of gum resin of *Boswellia serrata* in patients with chronic colitis. Planta Med 67(5):391–395. https://doi.org/10.1055/s-2001-15802

23. Safayhi H, Mack T, Sabieraj J, Anazodo MI, Subramanian LR, Ammon HP (1992) Boswellic acids: novel, specific, nonredox inhibitors of 5-lipoxygenase. J Pharmacol Exp Ther 261(3):1143–1146
24. Safayhi H, Rall B, Sailer ER, Ammon HP (1997) Inhibition by boswellic acids of human leukocyte elastase. J Pharmacol Exp Ther 281:460–463
25. Tausch L, Henkel A, Siemoneit U, Poeckel D, Kather N, Franke L, Hofmann B, Schneider G, Angioni C, Geisslinger G, Skarke C, Holtmeier W, Beckhaus T, Karas M, Jauch J, Werz O (2009) Identification of human cathepsin G as a functional target of boswellic acids from the anti-inflammatory remedy frankincense. J Immunol 183(5):3433–3442. https://doi.org/10.4049/jimmunol.0803574
26. Siemoneit U, Koeberle A, Rossi A, Dehm F, Verhoff M, Reckel S, Maier TJ, Jauch J, Northoff H, Bernhard F, Doetsch V, Sautebin L, Werz O (2011) Inhibition of microsomal prostaglandin E2 synthase-1 as a molecular basis for the anti-inflammatory actions of boswellic acids from frankincense. Br J Pharmacol 162(1):147–162. https://doi.org/10.1111/j.1476-5381.2010.01020.x
27. Amiri MS, Mohammadzadeh V, Yazdi MET, Barani M, Rahdar A, Kyzas GZ (2021) Plant-based gums and mucilages applications in pharmacology and nanomedicine: a review. Molecules 26(6):1770. https://doi.org/10.3390/molecules26061770
28. Kabir SF, Rahman A, Yeasmin F, Sultana S, Masud RA, Kanak NA, Haque P (2022) Chapter one—Occurrence, distribution, and structure of natural polysaccharides. In: Radiation-processed polysaccharides emerging roles in agriculture, pp 1–27
29. Purohit P, Bhatt A, Mittal RK, Abdellattif MH, Farghaly TA (2023) Polymer Grafting and its chemical reactions. Front Bioeng Biotechnol 10:1044927. https://doi.org/10.3389/fbioe.2022.1044927
30. Kumar D, Pandey J, Raj V, Kumar P (2017) A Review on the modification of polysaccharide through graft copolymerization for various potential applications. Open Med Chem J 11:109–126. https://doi.org/10.2174/1874104501711010109
31. Verma A, Gautam SP, Bansal KK, Prabhakar N, Rosenholm JM (2019) Green nanotechnology: advancement in phytoformulation research. Medicines (Basel) 6(1):39. https://doi.org/10.3390/medicines6010039
32. Namdarian P, Zamanian A, Asefnejad A, Saeedifar M (2018) Preparation and evaluation of olibanum extracts and determine their biocompatibility. RJPBCS 9(1):505–514
33. Liu J, Cui L, Losic D (2013) Graphene and graphene oxide as new nanocarriers for drug delivery applications. Acta Biomater 9(12):9243–9257. https://doi.org/10.1016/j.actbio.2013.08.016
34. Verma S, Tonk RK, Albratty M, Alhazmi HA, Najmi A, Kumar R, Kumar M, Taleuzzaman M, Swami G, Alam MS (2022) Design and evaluation of sustained release mucoadhesive film of sumatriptan succinate containing grafted co-polymer as the platform. Saudi Pharm J 30(11):1527–1537. https://doi.org/10.1016/j.jsps.2022.07.014
35. Beck-Broichsitter M, Lebhardt ERT, Wang X, Kissel T (2010) Preparation of nanoparticles by solvent displacement for drug delivery: a shift in the "ouzo region" upon drug loading. Eur J Pharm Sci 41:244–253. https://doi.org/10.1016/j.ejps.2010.06.007
36. Rohilla S, Awasthi R, Mehta M, Chellappan DK, Gupta G, Gulati M, Singh SK, Anand K, Oliver BG, Dua K, Dureja H (2022) Preparation and evaluation of gefitinib containing nanoliposomal formulation for lung cancer therapy. BioNanoSci 12:241–255. https://doi.org/10.1007/s12668-022-00938-6
37. Dinari A, Mortazavi Farsani SS, Mohammadi S, Najafi F, Abdollahi M (2020) Facile method for morphological characterization at nano scale. Iran J Biotechnol 18(3):e2645. https://doi.org/10.30498/IJB.2020.2645
38. Chan Y, Ng SW, Chellappan DK, Madheswaran T, Zeeshan F, Kumar P, Pillay V, Gupta G, Wadhwa R, Mehta M, Wark P (2020) Celastrol-loaded liquid crystalline nanoparticles as an anti-inflammatory intervention for the treatment of asthma. Int J Polym Mater. https://doi.org/10.1080/00914037.2020.1765350
39. Ni XL, Chen LX, Zhang H, Yang B, Xu S, Wu M, Liu J, Yang LL, Chen Y, Fu SZ, Wu JB (2017) *In-vitro* and *in-vivo* antitumor effect of gefitinib nanoparticles on human lung cancer. Drug Deliv 24(1):1501–1512. https://doi.org/10.1080/10717544.2017.1384862
40. Zhou X, Huang D, Wang R, Wu M, Zhu L, Peng W, Tu H, Deng X, Zhu H, Zhang Z, Wang X, Cao X (2021) Targeted therapy of rheumatoid arthritis via macrophage repolarization. Drug Deliv 28(1):2447–2459. https://doi.org/10.1080/10717544.2021.2000679
41. Fu Y, Lin Q, Gong T, Sun X, Zhang ZR (2016) Renal-targeting triptolide-glucosamine conjugate exhibits lower toxicity and superior efficacy in attenuation of ischemia/reperfusion renal injury in rats. Acta Pharmacol Sin 37(11):1467–1480. https://doi.org/10.1038/aps.2016.44
42. Jankowska-Kieltyka M, Roman A, Mikrut M, Kowalska M, van Eldik R, Nalepa I (2021) Metabolic response of RAW 264.7 sstter. Toxics 9(9):205. https://doi.org/10.3390/toxics9090205
43. Wang Q, Jiang H, Li Y, Chen W, Li H, Peng K, Zhang Z, Sun X (2017) Targeting NF-kB signaling with polymeric hybrid micelles that co-deliver siRNA and dexamethasone for arthritis therapy. Biomaterials 122:10–22. https://doi.org/10.1016/j.biomaterials.2017.01.008
44. Panwar P, Pandey B, Lakhera PC, Singh KP (2010) Preparation, characterization, and *in-vitro* release study of albendazole-encapsulated nanosize liposomes. Int J Nanomed 5:101–108. https://doi.org/10.2147/ijn.s8030
45. Zhou X, Cao X, Tu H, Zhang ZR, Deng L (2019) Inflammation-targeted delivery of celastrol via neutrophil membrane-coated nanoparticles in the management of acute pancreatitis. Mol Pharm 16(3):1397–1405. https://doi.org/10.1021/acs.molpharmaceut.8b01342
46. Bairwa K, Jachak SM (2016) Nanoparticle formulation of 11-keto-b-boswellic acid (KBA): anti-inflammatory activity and *in-vivo* pharmacokinetics. Pharm Biol 54(12):2909–2916. https://doi.org/10.1080/13880209.2016.1194437
47. Soumya RS, Ghosh S, Abraham ET (2010) Preparation and characterization of guar gum nanoparticles. Int J Biol Macromol 46(2):267–269. https://doi.org/10.1016/j.ijbiomac.2009.11.003
48. Farooq M, Sagbas S, Sahiner M, Siddiq M, Turk M, Aktas N, Sahiner N (2017) Synthesis, characterization and modification of gum arabic microgels for hemocompatibility and antimicrobial studies. Carbohydr Polym 156:380–389
49. Aamir M, Farooq M, Ambreen J, Ahmad N, Iqbal M, Haleem A, Saeed S, Shah A, Siddiq M (2019) Synthesis and characterization of gum arabic microgels stabilizing metal based nanocatalysts for ultrafast catalytic reduction of 4-nitrophenol at ambient conditions. J Environ Chem Eng 7(4):103280. https://doi.org/10.1016/j.jece.2019.103280

Publisher's Note